# Growth inhibition by STI571 in combination with radiation in human chronic myelogenous leukemia K562 cells

**Florence Huguet,[1,2,4] Nicole Giocanti,[1,2] Christophe Hennequin,[1,2,5] Martine Croisy,[1,3] Emmanuel Touboul,[4] and Vincent Favaudon[1,2]**

[1]Institut Curie, Centre de Recherche; [2]Institut National de la Santé et de la Recherche Médicale, U612; [3]Centre National de la Recherche Scientifique, UMR176, Orsay, France; and [4]AP-HP, Hôpital Tenon, Service d'Oncologie-Radiothérapie; and [5]AP-HP, Hôpital Saint Louis, Service de Cancérologie-Radiothérapie, Paris, France

## Abstract

**Altered radiation responses by STI571 (Imatinib, Glivec), a specific inhibitor of the tyrosine kinase activity of Bcr-Abl, was assessed in K562 chronic myelogenous leukemia cells using growth inhibition and colony formation assays. Flow cytometry, Western blotting, and microscope observation were used to determine cell cycle redistribution, erythroid differentiation, apoptosis, necrosis, senescence, and expression and phosphorylation of effectors downstream from Bcr-Abl as endpoints. STI571 ($\geq$24-h contact) retarded the growth of K562 cells and elicited reduction in the $G_2$-phase content due to an efficient arrest in early S phase rather than to the disruption of the $G_2$ checkpoint as confirmed by analysis of Lyn and CDK1 phosphorylation. STI571 brought about the inhibitory dephosphorylation of Bcr-Abl and STAT5, but the expression of DNA-PKcs and Rad51 was unaffected and the interaction between radiation and STI571 was strictly additive with regard to induction of apoptosis. Overall STI571 interacted cooperatively with radiation to retard the growth of K562 cells but did not affect intrinsic radiosensitivity. However, STI571 and radiation acted antagonistically with each other with regard to induction of senescence and erythroid differentiation. [Mol Cancer Ther 2008;7(2):398–406]**

Received 8/30/07; accepted 12/19/07.

**Grant support:** Fondation pour la Recherche Médicale (F. Huguet), Institut National de la Santé et de la Recherche Médicale, and Institut Curie.

The costs of publication of this article were defrayed in part by the payment of page charges. This article must therefore be hereby marked *advertisement* in accordance with 18 U.S.C. Section 1734 solely to indicate this fact.

**Note:** F. Huguet and N. Giocanti equally contributed to this study.

**Requests for reprints:** Vincent Favaudon, Institut National de la Santé et de la Recherche Médicale U612, Institut Curie-Recherche, Bât., 110-112, Centre Universitaire, 91405 Orsay Cedex, France.
Phone: 33-169863188; Fax: 33-169863187.
E-mail: vincent.favaudon@curie.fr



doi:10.1158/1535-7163.MCT-07-2023

## Introduction

c-Abl is a 145-kDa nonreceptor tyrosine kinase involved in a variety of cellular processes, including regulation of the cell cycle, actin organization, transduction of mitogenic signals, differentiation, and response to genotoxic stress (1, 2). Loss of c-Abl regulation may be oncogenic. Indeed, in pluripotent hematopoietic stem cells, the reciprocal t(9; 22)(q34; 11) chromosomal translocation generates the Philadelphia chromosome (3) and results in the fusion of the *BCR* and *ABL* genes. This translocation is the hallmark of chronic myelogenous leukemia (CML) and provided the first example of a specific genetic change associated with human cancer. *BCR-ABL* encodes a $p210^{Bcr\text{-}Abl}$ chimeric protein in which the Abl tyrosine kinase activity is constitutively turned on by dimerization-induced, intermolecular autophosphorylation (2, 4).

Multiple signaling proteins have been shown to interact with Bcr-Abl through various functional domains and/or to become phosphorylated in Bcr-Abl-expressing cells (5). These include Ras, mitogen-activated protein kinase, phosphatidylinositol-3-kinase, Akt, Jnk, Src family kinases, and their respective downstream targets as well as transcription factors, such as the signal transducers and activators of transcription (STAT), nuclear factor-κB, and Myc (6–12). In addition, the activation of STAT5 and the phosphatidylinositol-3-kinase pathway by Bcr-Abl may mediate inhibition of apoptosis via up-regulation of Bcl-2 expression and phosphorylation of the proapoptotic protein Bad (13).

Whether Bcr-Abl affects on the DNA damage and repair capacity of cells is a matter of controversy. It has been proposed that Bcr-Abl induces resistance to DNA-nicking agents via protection from apoptosis, prolongation of the $G_2$ checkpoint, and stimulation of DNA repair (14, 15). Bcr-Abl has also been reported to promote the expression of the homologous recombination effector Rad51 (16). Other authors, however, did not reach the same conclusions (17). Alternative mechanisms, including the Bcr-Abl-dependent down-regulation of the expression of the nonhomologous end-joining kinase DNA-PKcs (18) and the homologous recombination effector BRCA1 (19), have been proposed. All these pathways are liable to be altered by STI571 (Imatinib, Glivec), a 2-phenylaminopyrimidine derivative that acts as a specific inhibitor of Bcr-Abl. STI571 actually competes with ATP for the binding site at the SH1 catalytic domain of Bcr-Abl (20, 21) and inhibits Bcr-Abl autophosphorylation, thus maintaining the kinase in an inactive conformation. STI571 has proven its efficiency in CML (22) and is nowadays the standard treatment in this disease.

Combination of STI571 and radiation has been attempted in non-Bcr-Abl cells. The results are controversial. Uemura et al. (23) found no evidence of a radiosensitizing effect in U937 leukemia cells. In contrast, Russell et al. (24) and

Podtcheko et al. (25) reported that STI571 potentiates radiation-induced cell kill at high drug concentration in glioma and anaplastic thyroid cancer cells, respectively. The purpose of the present study was to assess the effect of STI571 on the radiation response in K562 CML cells expressing Bcr-Abl using growth inhibition, colony-forming ability, peroxidative metabolism, erythroid differentiation, apoptosis, senescence, and cell cycle progression as endpoints. The results show that in K562 cells STI571 cooperates with radiation to repress cell growth in a strictly additive way.

## Materials and Methods

### Reagents

4-(4-Methylpiperazin-1-ylmethyl)-*N*-[4-methyl-3-[4-(3-pyridyl)pyrimidin-2-ylamino]phenyl] benzamide (STI571) was synthesized according to Zimmermann et al. (26, 27) with slight modifications. Briefly, commercial *p*-toluic acid methyl ester was brominated with *N*-bromosuccinimid. The bromomethylated compound was coupled with *N*-methylpiperazine and the resulting ester was directly condensed with 4-methyl-*N*-3(4-pyridin-3-yl-pyrimidin-2-yl)-benzene-1,3-diamine using trimethylaluminum in dichloromethane. Purification by flash chromatography yielded the pure compound in 85% yield. Purity of STI571 was confirmed by TLC and nuclear magnetic resonance analysis.

Aliquots of STI571 were dissolved in pure DMSO and stored as a 10 mmol/L stock solution at −20°C. Dilutions were made daily in growth medium. The final concentration of DMSO was ≤0.5% so as not to alter cell growth or radiation responses. All experiments were done in dim light to avoid the photodegradation of the drug.

### Cell Line and Cell Culture

The human CML, Bcr-Abl-expressing cell line K562 (ATCC CCL-243) was kindly provided by Dr. Philippe Rousselot (Service d'Immunologie Clinique, Hôpital Saint-Louis) and maintained in RPMI 1640 supplemented with Glutamax I, penicillin, streptomycin, and 10% FCS at 37°C with 5% $CO_2$. K562 cells express high levels of Bcr-Abl and are mutated for p53 (28).

### Irradiation of Cells

Irradiation without or with concomitant exposure to STI571 was done at room temperature using a $^{137}$Cs γ-ray, IBL-637 irradiator (CIS-Biointernational) at a dose rate of 1.15 Gy/min. Each measurement was done in duplicate or triplicate. The relative cell growth or colony count was fitted to the classic linear-quadratic equation,

$$\ln S = -\alpha D - \beta D^2 \quad (1)$$

where $S$ is the growth or surviving fraction, $D$ is the radiation dose, and $\alpha$ and $\beta$ are adjustable variables characterizing radiosensitivity in the low ($\alpha$) and high ($\beta$) dose ranges of radiation, respectively. Calculations were made through nonlinear least-squares regression, taking all data points into account, using Kaleidagraph software (Synergy Software).

### Western Immunoblotting

Nuclear and cytoplasmic extracts were prepared each from $2 \times 10^7$ cells with protease and phosphatase inhibitors as described (29). Total extracts were made using M-PER reagent (Pierce) with protease and phosphatase inhibitors (Sigma-Aldrich). Proteins were titrated by the Bradford method using the Bio-Rad protein assay. Cell extracts were boiled in Laemmli loading buffer and separated on 5% (DNA-PKcs), 7.5% (Bcr-Abl, STAT5, and Lyn), or 10% (Rad51 and CDK1) SDS-PAGE gel. Proteins were transferred to nitrocellulose membranes (Schleicher & Schuell) and blocked for 1 h in 5% bovine serum albumin in TBST at 37°C. Membranes were subsequently incubated with primary monoclonal antibodies overnight at 4°C in TBST buffer, washed for 1 h, and incubated with horseradish peroxidase–conjugated secondary antibodies (Jackson ImmunoResearch Laboratories) in TBST buffer and revealed with an enhanced chemiluminescence detection kit (GE Healthcare-Amersham Biosciences). Nitrocellulose membranes were rehybridized with anti-α-tubulin antibody (Sigma-Aldrich). For immunoprecipitates, calibration of protein loading was made by scanning SDS-PAGE gels after Coomassie blue staining. Densitometric analysis was done using QuantityOne software (Bio-Rad).

### Immunodetection of CDK1 and p-Tyr$^{15}$-CDK1

Because antibodies directed against CDK1 (Cdc2) cross-react with other CDKs in Western blots, the analysis of CDK1 expression and Tyr$^{15}$ phosphorylation was carried out using CDK1 immunoprecipitates. Nuclear extracts were prepared in lysis buffer containing 50 mmol/L HEPES, 100 mmol/L NaCl, 1 mmol/L EDTA, 1 mmol/L EGTA, and 0.5% NP40 (pH 7.0) plus protease and phosphatase inhibitors. Three hundred microliters of the extract (250 μg protein) were incubated with 3 μL monoclonal mouse anti-Cdc2 (POH1, Cell Signaling Technology) at 4°C overnight with gentle rocking. Protein G-Sepharose beads (20 μL of 50% bead slurry) were added to the lysate and incubated for 4 h at 4°C on a rotator. The immunoprecipitates were washed four times with lysis buffer. The pellets were resuspended in 20 μL of 2× SDS loading buffer. Immunoprecipitates were separated by 12% SDS-PAGE and detected by chemiluminescence using monoclonal or polyclonal antibodies to Cdc2 and p-Tyr$^{15}$-Cdc2 (1:100 dilution; Cell Signaling Technology). GST-Cdc2 fusion protein and SK-N-MC total cell extracts treated with hydroxyurea (3 mmol/L, 24 h) were used as negative and positive controls, respectively.

### Annexin V Assay

Determination of apoptosis and necrosis was done using an Annexin V-FITC kit (Calbiochem). Briefly, $10^6$ cells were suspended in 1 mL ice-cold binding buffer [10 mmol/L HEPES, 150 mmol/L NaCl, 2.5 mmol/L $CaCl_2$, 1 mmol/L Mg $Cl_2$, 4% BSA (pH 7.4)]. Ten microliters of media binding buffer and 1.25 μL Annexin V-FITC antibody (Calbiochem) were added to 500 μL of the cell suspension for 15 min at room temperature in the dark. Cells were harvested by centrifugation and resuspended in 0.5 mL ice-cold binding buffer. Annexin V-FITC–labeled cells were analyzed

immediately using a FACStar PLUS cytofluorometer (Becton-Dickinson Biosciences). Propidium iodide (10 μL; 30 μg/mL in PBS) was subsequently added to allow discrimination between apoptotic (propidium iodide–negative) and necrotic (propidium iodide–positive) cells among the Annexin V–positive cells, and both propidium iodide and FITC fluorescence was determined by fluorescence-activated cell sorting. Signal analysis was carried out using CellQuest Pro software (Becton-Dickinson Biosciences).

### Analysis of DNA Fragmentation by Flow Cytometry (sub-$G_1$)

The hypodiploid (sub-$G_1$) fraction was measured using fluorescence-activated cell sorting analysis of propidium iodide–stained cells after overnight fixation with cold 70% ethanol. The sub-$G_1$ region was determined by a gate on the DNA content histogram excluding cell debris.

### Glycophorin A Assay

The expression of glycophorin A, a sialoglycoprotein present at the surface of human RBCs and erythroid precursors, was detected by direct immunofluorescence according to Kawano et al. (30). Briefly, $10^6$ K562 cells that had been exposed or not to STI571, radiation, or a combination of both were harvested, washed once with PBS supplemented with 2% FCS, and incubated in the dark (45 min, 4°C) with a monoclonal antibody directed against human glycophorin A following the manufacturer's instructions (PharMingen). After three washes with PBS containing 2% FCS, the cells were analyzed by flow cytometry. Mouse IgG antibody was used as isotype negative control.

### β-Galactosidase Staining and Determination of Senescent Cells

See Supplementary Material.[6]

### Cell Cycle Analysis

The effect of STI571 and/or radiation on the cell cycle distribution and progression of cells through S phase was monitored by dual-variable flow cytometry using a FACStar PLUS cytofluorometer as above. Pulse-chase labeling of K562 cells by bromodeoxyuridine (10-30 μmol/L, 10-20 min, 37°C) was done ahead of or following exposure to radiation and/or STI571 (see text and figure legends for details). Cells were finally harvested by centrifugation, washed once with ice-cold PBS, and fixed in 70% ice-cold ethanol. Treatment of fixed cells and data acquisition were carried out as described previously (31). Data analysis was done with CellQuest Pro software (Becton-Dickinson Biosciences).

## Results

### Effect of STI571 and Radiation on K562 Cell Growth and Survival

STI571 induced a time- and concentration-dependent inhibition of cell proliferation (Fig. 1). After 72-h contact, the amount of drug that reduced cell growth to 50% of that in controls ($IC_{50}$) was 0.14 ± 0.01 μmol/L. This value is in close agreement with those determined by other authors using a similar assay (32, 33). Past 48-h incubation, a drop in the cell count was observed at the highest drug concentrations used, suggesting a cytotoxic effect. This effect correlated with erythroid differentiation, a phenomenon described previously by Jacquel et al. (34). Indeed, STI571 generated tiny, hemoglobin-positive cells that expressed the same level of glycophorin A as undifferentiated cells but incorporated 10-fold as much propidium iodide (Fig. 2) and have proven unable to resume growth after drug removal.

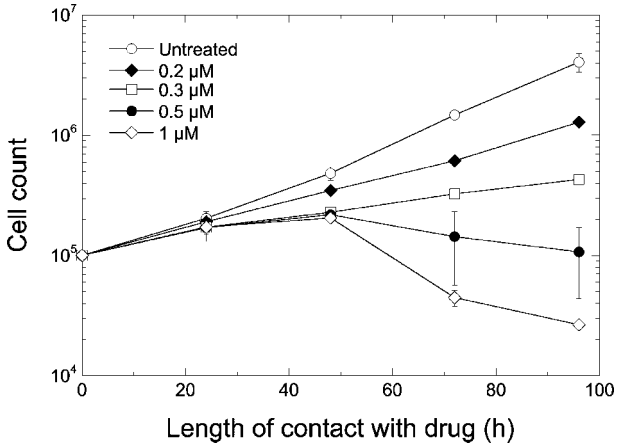


**Figure 1.** Time and dose dependence of growth inhibition by STI571. K562 cells were seeded at a constant density ($10^5$ cells in 8 mL medium, 25-$cm^2$ flasks) and incubated with STI571 for the time and concentration indicated. Every 24 h, cells were resuspended by mild agitation, an aliquot was withdrawn, and cells were counted in a hemocytometer. Bars, SD determined over three independent measurements.

For determination of the effect of combined treatment on cell growth, K562 cells were first incubated with STI571 for 24 h before irradiation. The results are shown in Fig. 3A. The growth curves obtained in the absence of STI571 fitted the linear-quadratic model [Eq. (1); see Materials and Methods]. In combination with radiation, STI571 brought about suppression of the $\beta$ variable together with a 2.1-fold increase of the $\alpha$ variable, suggesting radiosensitization in the low-dose range of radiation. Interestingly, radiation antagonized STI571-induced erythroid differentiation under similar conditions (Fig. 2).

For clonogenic assays, K562 cells were harvested at the end of treatment, freed from drug, and grown in semisolid medium. Reduction of the radiation susceptibility by a factor of 1.6 among drug survivors, specifically in the low-dose range of radiation was experienced in this assay (Fig. 3B).

In a third experiment, STI571 was introduced shortly after irradiation and was left in the medium for a maximum of 48 h. Under these conditions, we observed the same effect as in the first growth assay, that is, suppression of the quadratic component characteristic of radiation response together with a substantial increase of the $\alpha$ variable that was already apparent after 24 h contact with drug (Fig. 3C).

[6] Supplementary material for this article is available at Molecular Cancer Therapeutics Online (http://mct.aacrjournals.org/).

In summary, the comparison of growth and clonogenic experiments shows that STI571 is able to induce a cytotoxic effect likely to parallel erythroid differentiation but does not interfere substantially with the lethal effect of radiation, although a moderate radioprotecting effect was observed at low radiation dose in the clonogenic assay. At particular times past radiation exposure, however, the growth inhibitory effect of the drug resulted in suppression of the quadratic component ($\beta$) together with a substantial increase of the $\alpha$ variable characterizing response in the low-dose range of radiation.

### Radio-Induced Apoptosis and Necrosis without and with STI571

Apoptosis and necrosis of K562 cells were assessed by flow cytometric analysis of the sub-$G_1$ DNA fragments and Annexin V binding in cells exposed to 4 Gy alone, 0.3 μmol/L STI571 alone, and a combination of both. The susceptibility to STI571-induced apoptosis was in good agreement with Jacquel et al. (34). From both methods, the interaction between radiation and drug appeared to be purely additive with respect to the level of apoptosis (Fig. 4). Based on the DNA content, the necrosis index was below 1% under these conditions. However, necrosis was more pronounced than apoptosis at high concentrations of STI (14% for 1 μmol/L STI571, 20% for 10 μmol/L STI571, 72-h contact) in agreement with Okada et al. (35).

To extend these observations, Bcr-Abl and STAT5 expression and phosphorylation were analyzed by Western blot. Indeed, the phosphorylated form of STAT5 reportedly imparts sustained resistance to DNA damage-induced apoptosis (7) via up-regulation of the transcription of the antiapoptotic Bcl-$X_L$ protein (36). No significant change of Bcr-Abl and STAT5 expression was observed following radiation, STI571, or a combination of both. In contrast, STI571 abolished Bcr-Abl and STAT5 phosphorylation independently of whether cells were irradiated or not (Fig. 5).

### Radio-Induced Senescence without and with STI571

Ionizing radiation induced senescence-like changes in K562 cells exposed to radiation. Indeed, after 5-day incubation, a substantial part of irradiated cells underwent phenotypic changes characteristic of senescence, associated with β-galactosidase staining. At the concentration used, STI571 alone did not induce such changes. In combination with radiation, STI571 overcame the effect of radiation and abolished radiation-induced formation of β-galactosidase-positive cells to near completion (see Supplementary Material).

### Cell Cycle Studies

The time dependence of cell cycle disruption by radiation (6 Gy), STI571 (0.3 or 1 μmol/L), and a combination of both was investigated by flow cytometry for up to 72 h following initial treatment. The results are shown in Fig. 6.

Radiation alone induced a depletion of the $G_1$- and S-phase compartments together with prolonged accumulation in the $G_2$ phase. The effect reached a maximum at ~12 h ($G_1$, $G_2$) to 24 h (S) after irradiation. STI571 (0.3 μmol/L) alone brought about a transient $G_1$-phase accumulation and S-phase depletion peaking at 12 h of contact with drug followed by a progressive decrease of the $G_1$- and $G_2$-phase content and accumulation in S phase. These effects were

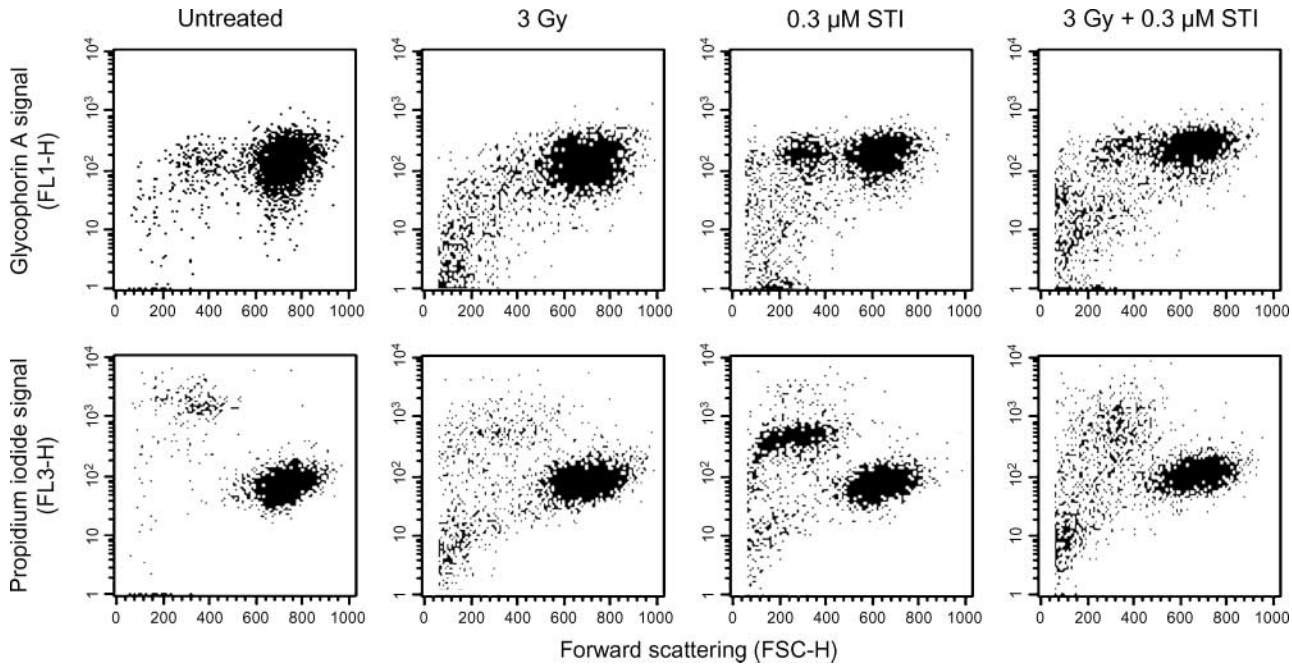


**Figure 2.** Flow cytometric analysis of erythroid differentiation in K562 cells by STI571 and radiation. Exponentially growing K562 cells were exposed or not to STI571 and/or γ-rays. In combined treatment, STI571 (48-h contact) was introduced 24 h before radiation and was present for an additional 24 h. At the end of incubation, cells were washed, fixed, exposed to anti-glycophorin A antibody then to a FITC-labeled secondary antibody, and analyzed by flow cytometry. The same samples were subsequently counterstained with propidium iodide to determine the DNA content.

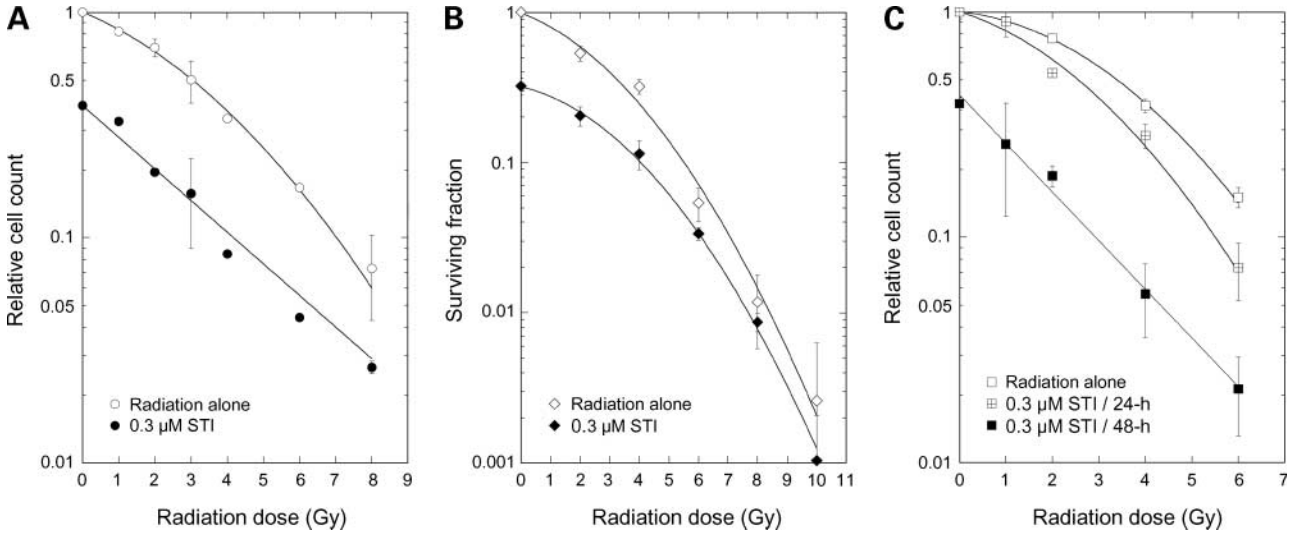


**Figure 3.** Effect of combined treatment with ionizing radiation and STI571 on cell growth and survival. **A,** growth assay, sequence drug → radiation → drug. Cells were irradiated without or with STI571. When present, the drug was introduced 24 h before irradiation and was left in the medium for a further 48 h. Cells were subsequently harvested by centrifugation, transferred to drug-free medium for 72 h, and counted. Radiation response in the absence of drug followed the linear-quadratic equation [Eq. (1); see Materials and Methods] with $\alpha = 0.152 \pm 0.017$ Gy$^{-1}$ and $\beta = 0.025 \pm 0.008$ Gy$^{-2}$. Radiation response in the presence of drug followed a single-exponential dose dependence with slope $\alpha = 0.323 \pm 0.031$ Gy$^{-1}$. The relative cell count at null radiation dose in the presence of STI571 was 0.385. **B,** clonogenic assay. Cells were incubated for 24 h in the absence or presence of STI571, irradiated or not, returned to the incubator for 48 h with or without STI571, then collected by centrifugation, washed twice with HBSS, counted, and plated (4,000 cells per 10-cm$^2$ dish) in semisolid medium using the methylcellulose technique (48). Colonies were scored under microscope examination after 12 days of growth. Found: $\alpha = 0.166 \pm 0.034$ Gy$^{-1}$ and $\beta = 0.045 \pm 0.009$ Gy$^{-2}$ in the absence of drug and $\alpha = 0.104 \pm 0.016$ Gy$^{-1}$ and $\beta = 0.045 \pm 0.005$ Gy$^{-2}$ in the presence of STI571. The drug surviving fraction at null radiation dose was 0.319. **C,** growth assay, sequence radiation → drug. STI571 was introduced shortly after irradiation and was present for 24 or 48 h. Cells were subsequently incubated in drug-free medium for 5 days and counted. For radiation alone, $\alpha = 0.0265 \pm 0.0038$ Gy$^{-1}$ and $\beta = 0.0484 \pm 0.0111$ Gy$^{-2}$. For 24-h incubation with STI, $\alpha = 0.144 \pm 0.077$ Gy$^{-1}$ and $\beta = 0.0498 \pm 0.0264$ Gy$^{-2}$. After 48-h incubation in the presence of STI, radiation response fitted a single exponential with slope $\alpha = 0.489 \pm 0.014$ Gy$^{-1}$; the growth fraction at null radiation dose was 0.429.

more pronounced in the presence of 1 μmol/L drug. In particular, 1 μmol/L drug abrogated the radio-induced $G_2$ block and elicited prolonged accumulation in S phase paralleling $G_1$-phase depletion.

Abolition of the $G_2$-phase arrest by caffeine has long been known to slow the progress of DNA repair and result in a radiosensitizing effect. We used two methods to determine whether a similar event could be induced by STI571 in

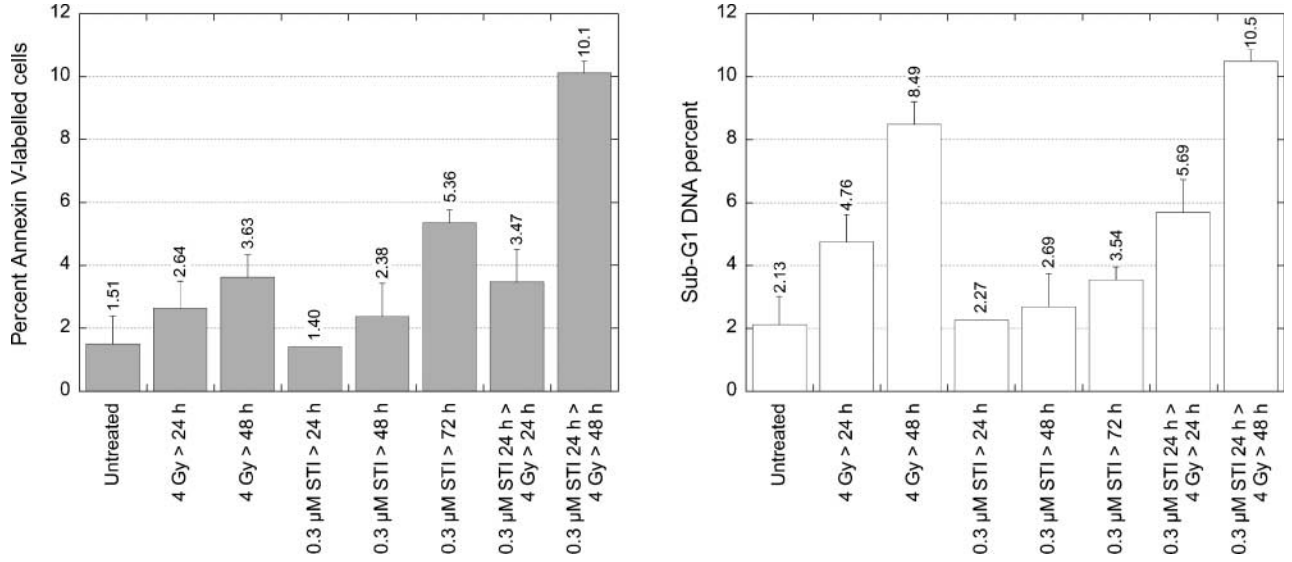


**Figure 4.** Determination of STI571-induced apoptosis and effect of drug on radio-induced apoptosis in K562 cells. Cells were exposed to radiation or drug, collected, and processed for Annexin V-FITC or sub-$G_1$ fragments determination by flow cytometry as indicated in the text. In combined treatment, STI571 was introduced 24 h before irradiation and was present for up to cell harvest.

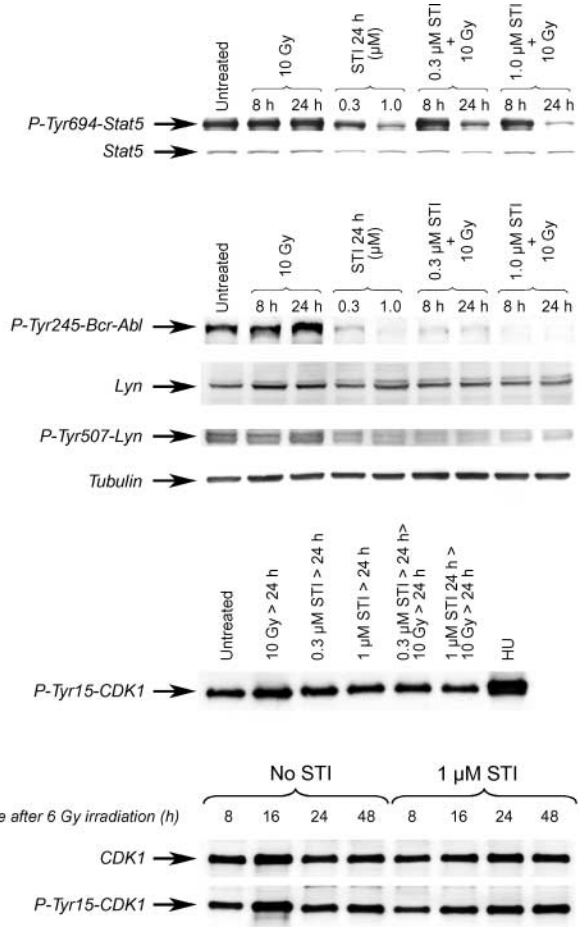


**Figure 5.** Western blot determination of the expression and phosphorylation of STAT5, CDK1, Bcr-Abl, and Lyn following radiation with or without STI571. Bcr-Abl, Lyn, and STAT5 were probed from total extracts (30 μg/lane). CDK1 was probed from immunoprecipitates prepared from nuclear extracts of K562 cells (see Materials and Methods). *HU*, treatment with hydroxyurea (3 mmol/L, 24 h). The antibodies used were mouse monoclonal antibody against STAT5 (Becton-Dickinson Biosciences) and rabbit polyclonal antibodies against p-Tyr$^{694}$-STAT5, Lyn, p-Tyr$^{507}$-Lyn, c-Abl (cross-reacting with Bcr-Abl), and p-Tyr$^{275}$-c-Abl (cross-reacting with p-Bcr-Abl; Cell Signaling Technology).

K562 cells. For this purpose, we analyzed (*a*) the pathway involved in the control of the $G_2$ transition through Tyr$^{15}$ phosphorylation of CDK1 (Cdc2) and (*b*) the cell cycle progress in cells that had been labeled with bromodeoxyuridine in S phase before exposure to drug or radiation.

**Control of the $G_2$-Phase Progression.** Loss of Bcr-Abl phosphorylation is expected to reduce the activity of the tyrosine kinase Lyn through Tyr$^{507}$ dephosphorylation (37). The phosphorylated form of Lyn has been involved in the control of Tyr$^{15}$ phosphorylation of CDK1, thus controlling the transit through late $G_2$ and mitosis (38). Exposure to STI571 was found to induce a loss of Lyn phosphorylation (Fig. 5), consistent with the lack of a radio-induced $G_2$ block in the presence of STI571 (Fig. 6). This study was completed by analysis of CDK1 expression and phosphorylation using immunoprecipitates. As expected, radiation alone elicited a transient increase of the nuclear content and phosphorylation of CDK1, peaking at ~16 h following radiation (Fig. 5). Preincubation (24 h) with 1 μmol/L STI571 prevented CDK1 phosphorylation, consistent with the flow cytometric analysis that showed a lack of accumulation of cells in $G_2$ under these conditions.

**Control of the S-Phase Progression.** From the data presented above, it may be inferred either that STI571 abrogates the radio-induced $G_2$ block through down-regulation of Lyn phosphorylation or that cells are blocked at an earlier stage.

To resolve this issue, the effect of STI571 and/or radiation on the relative movement of cells through S phase was analyzed in asynchronous K562 cells that had been pulse labeled with bromodeoxyuridine in S phase. Both STI571 and radiation slowed down the transit of cells through the S phase of the cell cycle. The combination of radiation and STI571 produced an additive effect (see Supplementary Material).

## Discussion

STI571 at high concentration has been reported to increase radiation susceptibility in glioblastoma cells both *in vitro* (24) and in mouse models (39, 40). This effect was assigned to disruption of an autocrine loop involved in phosphorylation (activation) of the platelet-derived growth factor receptor (39, 40) and was not observed in breast and colon cancer cells (40). At high enough concentrations to inhibit the activity of c-Abl, STI571 was able to potentiate radiation response in cells from anaplastic thyroid cancer (25). However, at concentrations achieving complete inhibition of Bcr-Abl but insufficient to depress c-Abl activity, STI571 did not alter the radiation response in normal bone marrow cells from BALB/c mice and in U937 human leukemia cells in a clonogenic assay *in vitro* (23). Here, we show that STI571 at cytostatic concentrations represses cell growth cooperatively with radiation in K562 CML cells but does not induce any significant change in radiation susceptibility, consistent with the fact that the expression of DNA-PKcs was not altered (see Supplementary Material).

STI571 at submicromolar concentration did not alter the expression of Bcr-Abl and STAT5 expression in K562 cells but abrogated the phosphorylation of Bcr-Abl-Tyr$^{245}$ and STAT5-Tyr$^{694}$, as also observed by others (34, 41) and independently of whether cells were irradiated or not. As the phosphorylated form of STAT5 imparts sustained resistance to DNA damage-induced apoptosis (7, 36), down-regulation of STAT5 phosphorylation would be expected to result in an enhanced susceptibility of K562 cells to apoptosis. However, although K562 cells showed time- and dose-dependent apoptosis in response to STI571 and radiation, as shown in Fig. 4, the drug did not potentiate radiation-induced apoptosis and the interaction between both modalities was strictly additive. The same result was obtained by Podtcheko et al. (25) using non-Bcr-Abl anaplastic thyroid cancer cells.

A substantial part of K562 cells exposed to radiation alone displayed phenotypic changes associated with the formation of β-galactosidase-positive cells (see Supplementary Material) typical of senescence-like, terminal growth arrest in nearly the same way as described for hydroxyurea treatment also in K562 cells (42). Surprisingly enough, STI571 acted antagonistically with radiation in this pathway. Symmetrically, in our hands, radiation antagonized drug-induced erythroid differentiation of K562 cells (Fig. 2). These results are at variance with those obtained at high drug concentration in the non-Bcr-Abl anaplastic thyroid cancer cells (25). One would tentatively propose to explain these differences that pathways of DNA damage response under control of the c-Abl tyrosine kinase are not operating in CML cells. Alternatively, inhibition of the catalytic activity of other tyrosine kinases, such as c-Kit or platelet-derived growth factor receptor, at concentrations 1 order of magnitude above those used in this study should also be taken into consideration.

Riordan et al. (43) and Jeong et al. (44) earlier reported that herbimycin A, an inhibitor of c-Abl and Bcr-Abl, increased the level of radiation-induced apoptosis in K562 cells. This effect was associated with the abrogation of the $G_2$ checkpoint (44). Actually, bypassing the $G_2$ checkpoint reduces the amount of DNA repair that can take place and leads to an increase of radiation susceptibility. To determine whether this effect occurred in K562 cells, we analyzed the effect of STI571 on the phosphorylation of Lyn, a member of the Src tyrosine kinase family. As a matter of fact, constitutive activation of Lyn through $Tyr^{507}$ phosphorylation is driven by Bcr-Abl (45). Lyn can also be activated by radiation and other DNA-damaging agents. p-$Tyr^{507}$-Lyn binds to and phosphorylates CDK1 on the $Tyr^{15}$ residue, and p-$Tyr^{15}$-CDK1 is necessary to block $G_2$-M progression (38). Although Lyn expression did not vary after radiation or prolonged exposure to STI571, Lyn phosphorylation slightly increased after radiation exposure and was abolished by STI571. Such inhibition of Lyn phosphorylation is sufficient to induce suppression of the radio-induced $G_2$ block. However, this explanation does not hold in the present case. Indeed, studies with pulse-chased bromodeoxyuridine-labeled cells showed that a short contact with STI571 lengthened S-phase progression (see Supplementary Material) but did not affect the duration of the $G_2$ block induced by radiation. On the other hand, prolonged exposure to 1 μmol/L STI571 resulted in the accumulation of cells in $G_1$ and in early S phase. This block was efficient enough to starve the $G_2$ compartment.

The ability of STI571 to induce transient accumulation in early S phase suggests that STI571 might be able to potentiate the cytotoxic effect of topoisomerase I and II poisons in c-Kit and platelet-derived growth factor receptor–expressing solid tumors, which are both targets

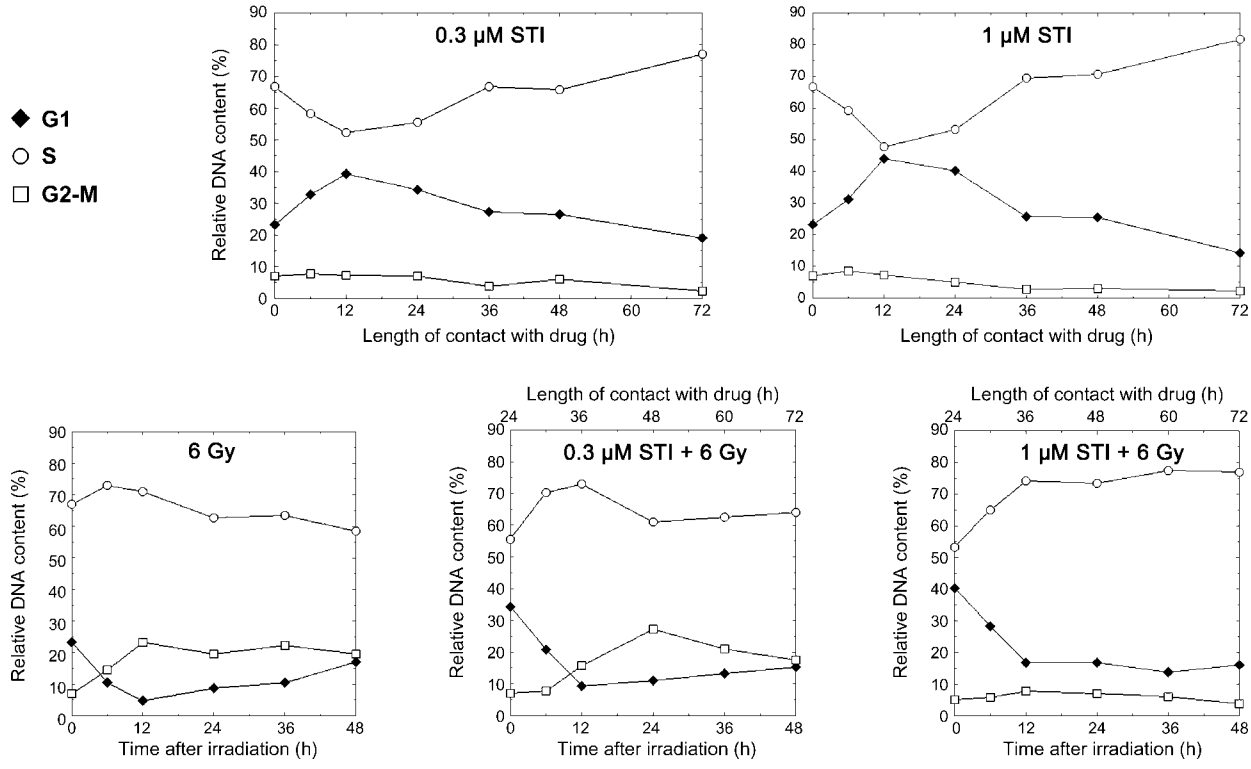


**Figure 6.** Altered cell cycle progression of growing K562 cells by STI571 and radiation. In combined treatment, cells were incubated with STI571 for 24 h before radiation. Cells were harvested at the times indicated, incubated with bromodeoxyuridine (10 μmol/L, 15 min) for S-phase DNA labeling, and processed (31) for flow cytometric analysis. For sake of clarity, the sub-$G_1$ fraction has not been shown on the diagram.

for STI571. Indeed, STI571 has been reported to act synergistically with etoposide and topotecan in small cell lung cancer xenografts (46). Moreover, in c-Kit-positive small cell lung cancer cells, STI571 was found to up-regulate topoisomerase I activity and potentiate induced cell kill by camptothecin derivatives (47). Clearly, the possibility of selective sensitization to S-phase targeting drugs by STI571 in Bcr-Abl, platelet-derived growth factor receptor, or c-Kit-expressing tumors warrants further investigation.

**Acknowledgments**

We thank Dr. Philippe Rousselot for the generous gift of K562 cells, Drs. Eric Deutsch (Institut Gustave-Roussy), Janet Hall and Frédérique Mégnin-Chanet (Institut Curie) for helpful discussion, and Danièle Rouillard for the flow cytometric analysis of the cell cycle.

**References**

**1.** Van Etten RA. Cycling, stressed-out and nervous: cellular functions of c-Abl. Trends Cell Biol 1999;9:179 – 86.

**2.** Hantschel O, Superti-Furga G. Regulation of the c-Abl and Bcr-Abl tyrosine kinases. Nat Rev Mol Cell Biol 2004;5:33 – 44.

**3.** Nowell PC, Hungerford DA. Chromosome studies on normal and leukemic human leukocytes. J Natl Cancer Inst 1960;25:85 – 109.

**4.** Van Etten RA. Mechanisms of transformation by the BCR-ABL oncogene: new perspectives in the post-Imatinib era. Leuk Res 2004;28 Suppl 1:21 – 8.

**5.** Deininger MW, Goldman JM, Melo JV. The molecular biology of chronic myeloid leukemia. Blood 2000;96:3343 – 56.

**6.** Sillaber C, Gesbert F, Frank DA, Sattler M, Griffin JD. STAT5 activation contributes to growth and viability in Bcr/Abl-transformed cells. Blood 2000;95:2118 – 25.

**7.** Hoover RR, Gerlach MJ, Koh EY, Daley GQ. Cooperative and redundant effects of STAT5 and Ras signaling in BCR/ABL transformed hematopoietic cells. Oncogene 2001;20:5826 – 35.

**8.** Xie S, Lin H, Sun T, Arlinghaus RB. Jak2 is involved in c-Myc induction by Bcr-Abl. Oncogene 2002;21:7137 – 46.

**9.** Kawauchi K, Ogasawara T, Yasuyama M, Ohkawa S. Involvement of Akt kinase in the action of STI571 on chronic myelogenous leukemia cells. Blood Cells Mol Dis 2003;31:11 – 7.

**10.** Chu S, Holtz M, Gupta M, Bhatia R. BCR/ABL kinase inhibition by Imatinib mesylate enhances MAP kinase activity in chronic myelogenous leukemia $CD34^+$ cells. Blood 2004;103:3167 – 74.

**11.** Parmar S, Katsoulidis E, Verma A, et al. Role of the p38 map kinase pathway in the generation of the effects of Imatinib mesylate (STI571) in BCR-ABL expressing cells. J Biol Chem 2004;279:25345 – 52.

**12.** Kharas MG, Fruman DA. ABL oncogenes and phosphoinositide 3-kinase: mechanism of activation and downstream effectors. Cancer Res 2005;65:2047 – 53.

**13.** Keeshan K, Cotter TG, McKenna SL. High Bcr-Abl expression prevents the translocation of Bax and Bad to the mitochondrion. Leukemia 2002;16:1725 – 34.

**14.** Slupianek A, Hoser G, Majsterek I, et al. Fusion tyrosine kinases induce drug resistance by stimulation of homology-dependent recombination repair, prolongation of G(2)/M phase, and protection from apoptosis. Mol Cell Biol 2002;22:4189 – 201.

**15.** Skorski T. BCR/ABL regulates response to DNA damage: the role in resistance to genotoxic treatment and in genomic instability. Oncogene 2002;21:8591 – 604.

**16.** Slupianek A, Schmutte C, Tombline G, et al. BCR/ABL regulates mammalian RecA homologs, resulting in drug resistance. Mol Cell 2001;8: 795 – 806.

**17.** Dierov J, Dierova R, Carroll M. BCR/ABL translocates to the nucleus and disrupts an ATR-dependent intra-S phase checkpoint. Cancer Cell 2004;5:275 – 85.

**18.** Deutsch E, Dugray A, Abdul-Karim B, et al. BCR-ABL down-regulates the DNA repair protein DNA-PKcs. Blood 2001;97:2084 – 90.

**19.** Deutsch E, Jarrousse S, Buet D, et al. Down-regulation of BRCA1 in BCR-ABL-expressing hematopoietic cells. Blood 2003;101: 4583 – 8.

**20.** Buchdunger E, Zimmermann J, Mett H, et al. Inhibition of the Abl protein-tyrosine kinase *in vitro* and *in vivo* by a 2-phenylaminopyrimidine derivative. Cancer Res 1996;56:100 – 4.

**21.** Schindler T, Bornmann W, Pellicena P, Miller WT, Clarkson B, Kuriyan J. Structural mechanism for STI-571 inhibition of Abelson tyrosine kinase. Science 2000;289:1938 – 42.

**22.** O'Brien SG, Guilhot F, Larson RA, et al. Imatinib compared with interferon and low-dose cytarabine for newly diagnosed chronic-phase chronic myeloid leukemia. N Engl J Med 2003;348:994 – 1004.

**23.** Uemura N, Griffin JD. The ABL kinase inhibitor STI571 does not affect survival of hematopoietic cells after ionizing radiation. Blood 2000; 96:3294 – 5.

**24.** Russell JS, Brady K, Burgan WE, et al. Gleevec-mediated inhibition of Rad51 expression and enhancement of tumor cell radiosensitivity. Cancer Res 2003;63:7377 – 83.

**25.** Podtcheko A, Ohtsuru A, Namba H, et al. Inhibition of ABL tyrosine kinase potentiates radiation-induced terminal growth arrest in anaplastic thyroid cancer cells. Radiat Res 2006;165:35 – 42.

**26.** Zimmermann J, Buchdunger E, Mett H, Meyer T, Lydon NB, Traxler P. Phenylamino-pyrimidine (PAP)-derivatives: a new class of potent and highly selective PDGF-receptor autophosphorylation inhibitors. Bioorg Med Chem Lett 1996;6:1221 – 6.

**27.** Zimmermann J, Buchdunger E, Mett H, Meyer T, Lydon NB. Potent and selective inhibitors of the Abl-kinases: phenylamino-pyrimidine (PAP)-derivatives. Bioorg Med Chem Lett 1997;7:187 – 92.

**28.** Drexler HG, MacLeod RA, Uphoff CC. Leukemia cell lines: *in vitro* models for the study of Philadelphia chromosome-positive leukemia. Leuk Res 1999;23:207 – 15.

**29.** Piret B, Schoonbroodt S, Piette J. The ATM protein is required for sustained activation of NF-κB following DNA damage. Oncogene 1999; 18:2261 – 71.

**30.** Kawano T, Horiguchi-Yamada J, Saito S, et al. Ectopic cyclin D1 expression blocks STI571-induced erythroid differentiation of K562 cells. Leuk Res 2004;28:623 – 9.

**31.** Demarcq C, Bastian G, Remvikos Y. BrdUrd/DNA flow cytometry analysis demonstrates *cis*-diamminedichloroplatinum (II)-induced multiple cell-cycle modifications on human lung carcinoma cells. Cytometry 1992; 13:416 – 22.

**32.** Yu C, Krystal G, Dent P, Grant S. Flavopiridol potentiates STI571-induced mitochondrial damage and apoptosis in BCR-ABL-positive human leukemia cells. Clin Cancer Res 2002;8:2976 – 84.

**33.** Park J, Kim S, Oh C, Yoon SS, Lee D, Kim Y. Differential tyrosine phosphorylation of leukemic cells during apoptosis as a result of treatment with Imatinib mesylate. Biochem Biophys Res Commun 2005;336: 942 – 51.

**34.** Jacquel A, Herrant M, Legros L, et al. Imatinib induces mitochondria-dependent apoptosis of the Bcr-Abl-positive K562 cell line and its differentiation toward the erythroid lineage. FASEB J 2003; 17:2160 – 2.

**35.** Okada M, Adachi S, Imai T, et al. A novel mechanism for Imatinib mesylate-induced cell death of BCR-ABL-positive human leukemic cells: caspase-independent, necrosis-like programmed cell death mediated by serine protease activity. Blood 2004;103:2299 – 307.

**36.** Gesbert F, Griffin JD. Bcr/Abl activates transcription of the Bcl-X gene through STAT5. Blood 2000;96:2269 – 76.

**37.** Ptasznik A, Urbanowska E, Chinta S, et al. Crosstalk between BCR/ABL oncoprotein and CXCR4 signaling through a Src family kinase in human leukemia cells. J Exp Med 2002;196:667 – 78.

**38.** Kharbanda S, Saleem A, Yuan ZM, et al. Nuclear signaling induced by ionizing radiation involves colocalization of the activated p56/p53lyn tyrosine kinase with p34cdc2. Cancer Res 1996;56:3617 – 21.

**39.** Geng L, Shinohara ET, Kim D, et al. STI571 (Gleevec) improves tumor growth delay and survival in irradiated mouse models of glioblastoma. Int J Radiat Oncol Biol Phys 2006;64:263 – 71.

**40.** Holdhoff M, Kreuzer KA, Appelt C, et al. Imatinib mesylate radiosensitizes human glioblastoma cells through inhibition of platelet-derived growth factor receptor. Blood Cells Mol Dis 2005;34:181 – 5.

**41.** Jacobberger JW, Sramkoski RM, Frisa PS, et al. Immunoreactivity of

Stat5 phosphorylated on tyrosine as a cell-based measure of Bcr/Abl kinase activity. Cytometry 2003;54:75 – 88.

**42.** Park JI, Jeong JS, Han JY, et al. Hydroxyurea induces a senescence-like change of K562 human erythroleukemia cell. J Cancer Res Clin Oncol 2000;126:455 – 60.

**43.** Riordan FA, Bravery CA, Mengubas K, et al. Herbimycin A accelerates the induction of apoptosis following etoposide treatment or γ-irradiation of bcr/abl-positive leukaemia cells. Oncogene 1998;16:1533 – 42.

**44.** Jeong SJ, Jin YH, Moon CW, et al. Protein tyrosine kinase inhibitors modulate radiosensitivity and radiation-induced apoptosis in K562 cells. Radiat Res 2001;156:751 – 60.

**45.** Danhauser-Riedl S, Warmuth M, Druker BJ, Emmerich B, Hallek M. Activation of Src kinases p53/56lyn and p59hck by p210bcr/abl in myeloid cells. Cancer Res 1996;56:3589 – 96.

**46.** Decaudin D, de Crémoux P, Sastre X, et al. *In vivo* efficacy of STI571 in xenografted human small cell lung cancer alone or combined with chemotherapy. Int J Cancer 2005;113:849 – 56.

**47.** Maulik G, Bharti A, Khan E, Broderick RJ, Kijima T, Salgia R. Modulation of c-Kit/SCF pathway leads to alterations in topoisomerase-I activity in small cell lung cancer. J Environ Pathol Toxicol Oncol 2004;23: 237 – 51.

**48.** Aye MT, Seguin JA, McBurney JP. Erythroid and granulocytic colony growth in cultures supplemented with human serum lipoproteins. J Cell Physiol 1979;99:233 – 8.